1964

Solid-phase welding of nodular iron to low carbon steel.

Scott H. Carriere

Department:

SOLID-PHASE WELDING OF NODULAR IRON TO LOW CARBON STEEL

BY

SCOTT H. CARRIERE

A

THESIS

submitted to the faculty of the

UNIVERSITY OF MISSOURI AT ROLLA

in partial fulfillment of the requirements for the

Degree of

MASTER OF SCIENCE IN MECHANICAL ENGINEERING

Rolla, Missouri

1964

Approved by

Robert J. Wall (advisor) Lyman V. Francis

Peter Y. Hansen Ralph E. Schowalter

ABSTRACT

This paper presents an experimental investigation of the possibility of using solid-phase welding to join nodular iron to low carbon steel. Included is a review of available literature on solid-phase welding, tracing its origin from early Egypt to the present day. There was no previously reported work found on the welding of nodular iron to steel.

Experiments were performed to determine what temperature-pressure combination gave the greatest ultimate tensile strength These experiments resulted in the best welds being produced with an end load of 7000 pounds (35.700 psi) on a half inch diameter sample. The majority of these welds proved to have a strength of 90% to 95% of the base iron strength.

ACKNOWLEDGEMENTS

The author wishes to thank Professor R. V. Wolf for his suggestions, assistance and criticisms during the development of this paper. Thanks go also to Mr. R. L. Wright for his assistance in producing the photomicrographs. Wells Manufacturing, Skokie, Illinois is also to be thanked for the donation of their 60-45-10 continuous cast nodular iron bar.

The author also wishes to acknowledge the financal assistance received from the Metallurgical Engineering Department in the form of a Graduate Assistantship.

TABLE OF CONTENTS

LIST OF ILLUSTRATIONS

LIST OF TABLES

I. INTRODUCTION

The purpose of the following work is to ascertain if solid-phase welding can be used to join nodular iron to low carbon steel. Previously the welding of iron to steel was thought to be unrealistic due to the difference in melting temperatures and the undesirable products formed in the weld zone. Because of this, brazing was used when the two metals were to be joined resulting in a joint which required special design considerations and usually exhibited lower strength than the base materials. In addition, brazing operations usually prove to be relatively slow production processes. Solid-phase welding shows a possible way to avoid the undesirables previously encountered and could prove to be of great use to designers in joining castings to rolled steel.

II. REVIEW OF LITERATURE

Solid-phase welding differs from the two more common methods of metallurgical joining, fusion welding and brazing or soldering, in that there is no liquid metal present during the joining process. Solid-phase welding has not been developed to as great an extent as the others even though it is the oldest of the three types (1)*. Iron was used in Egypt as early as 3000 B. C. This iron was prepared by producing a metal sponge and hammering it to weld the particles together. The product was often unsound and contained slag inclusions but excellent samples were occasionally produced. From this early time, until J. I. Desaguliers' demonstration for the Royal Society in 1724, there was no development or further usage (2). Desaguliers took two lead balls, on which a 3/4 inch flat had been cut, pressed these together with a twist and they were found to be joined. The joint strength was measured and although there was some scatter in the results, good bonds were produced, with some as strong as that of the base metal. In 1781, Achard, working with platinum sponge, used solid-phase welding. These experiments

---

*(1) All references are in the bibliography.

shortly resulted in the production of platinum by powder metallurgy methods (1). In spite of these early demonstrations, solid-phase bonding was limited to powder metallurgy until 1935 when the roll bonding of clad metals was first developed (2). The Second World War accelerated development and today it is widely accepted that most metals can be pressure welded. Large numbers of combinations of dissimilar metals can also be welded if they have reasonably similar coefficients of thermal expansion (3).

The ancient art of forge welding has sometimes been considered to be a special case of solid-phase welding (1). In this type of welding, low melting phases, which are liquid at the forge welding temperatures, are largely responsible for the bonding. The use of a flux increases the amount of liquid present and the hammering serves primarily to squeeze out the excess liquid. Upon inspection, a once molten zone can be found at the original interface, thus forge welding is not a form of true solid-phase welding (1).

The mechanism of bonding that is theorized by Kinzel (1) and upheld by Fine, Maack and Ozanick (4) and Holmes (5) is metallic cohesion. When two pieces of metal are brought into contact so the atoms of one are at a distance

of one lattice parameter from the second, atomic bonding is possible. The atoms will then diffuse across the interface in their natural movement from one lattice position to another creating the possibility of recrystallization, grain growth and overall coalescence. To obtain such spacing in practical applications, any surface film which may be present at the interface must be dispersed. It is usually possible by mechanical cleaning to remove all surface contamination except for an oxide layer which continues to reform.

For steel, Fine, Maack and Ozanick (4) and Kinzel (1) have presented a theory of oxygen diffusion from the weld interface into the base metal. The oxygen is dissolved in the base steel upon heating and if the temperature is held long enough it will diffuse from the area of high concentration, the weld interface, to one of lower concentration. Kinzel (1) presents a theoretical treatment to prove the complete diffusion of a 0.1 mm (0.004 inch) thick film held at 1000°C (1832°F) for 30 minutes. In these experiments a temperature of 1050°C (1922°F) was found to be about the minimum for good oxide dispersion in the time normally allowable. This diffusion was found by Fine, Maack and Ozanick (4) to take a considerable

length of time at an elevated temperature. The results show that the weld interface contained oxides even after 8 hours at 2300°F. Deformation of the weld interface can be used to help disperse this oxide layer and also promote diffusion.

Materials such as Aluminum which have a low solubility for oxygen depend on the mechanical dispersion of the oxide layer in order to promote welding. This dispersion of the oxide layer is promoted by the deformation of the weld interface. (5)(6)(7)(8) or by the use of ultrasonic vibrations (9).

Parameters which are considered to influence the quality of solid-phase welds are temperature, pressure, deformation, and surface condition (2). These are discussed in the following pages.

Temperature:

The main effects of elevated temperature are:

A. It may increase the dissolution of the oxygen from the oxide film, or evaporate the surface contaminants (1)(2)(3)(7)(8).

B. It increases atomic mobility which increases rates of diffusion. These are particulary pronounced at allotropic

transformation temperatures (1) and at recrystallization temperatures (2). Work using very low pressure and little deformation has shown bonding to commence close to the recrystallization temperature for a given metal (6).

C. It lowers the yield strength to zero at the recrystallization temperature. A low yield strength particularly allows plastic flow of surface roughness and increases the area of contact, decreasing interatomic distances across the interface (5).

Pressure:

Pressure has been considered by some investigators to be the most important parameter. Rollason (2) and McEwan (10) have shown in their works that increasing the pressure above that necessary to produce the threshold deformation increases the development of bonding.

Deformation:

The importance of deformation, once past the threshold deformation at which bonding first occurs, is in the production of fragmentation of the oxide film on the surface of the weld interface. This fragmentation increases the virgin metal available for welding (8)(7)(5)(10). The threshold deformation has been shown to decrease with increasing

temperatures due to increased atomic mobility (6)(11).

Surface Condition:

Surface condition has previously been discussed and can be seen to be of importance in the weldability of metals. The surface preparation that has proven to be the most useful is the mechanical removal of absorbed contaminants, but welding should be carried out immediately after treatment (7)(1)(4)(5)(6). Chemical removal of surface contaminants has been reported to be of less benefit (7).

Mc Ewan, working with solid-phase welding of pairs of dissimilar metals, divided his attention between four categories of paired materials; immiscible, partially miscible, miscible, and intermetallic forming (10). His results are as follows:

Immiscible metal pairs and those having limited solubility can be welded, and the welds are stable on subsequent heat treatment.

Miscible metals weld readily but on subsequent heat treatment at high temperature the bond may weaken owing to the formation of porosity. The most important factor

influencing the formation of porosity is that interdiffusion occurs at unequal rates in opposite directions across the interface.

With metal combinations that form intermetallic compounds, two types of behavior were observed, depending on whether or not the intermetallic layer possessed any ductility. A high bond strength is obtained with thin brittle layers and any fracturing of the intermetallic layer occurs across it without affecting the bond across the interface. With a thick brittle intermetallic layer, fractures are at random, resulting in its crumbling and the splitting of the composite. The critical thickness at which this transition takes place varies with the system. If the layer is ductile, the bond strength is strong, regardless of its thickness at the interface, and fractures occur in the weaker of the base metals.

Solid-phase or pressure welding is used today in many industrial applications. A few of these are: boiler tubes, heat exchangers, roll bonding of clad metals, aircraft landing gear, pipe line welding of from two to 24 inch diameter pipe, railroad rails, oil well tool joints and sheathing of cable (11)(12)(13)(14)(15). The aero-space industries are also finding it necessary

to investigate solid-phase welding for spaceborne bearings, slip rings, electrical contacts, and other metal surfaces which unintentionally bond together in the vacuum of space. With the ultraclean metals used in these components an oxide layer does not form in this vacuum and bonding has a tendency to occur (16).

III. DISCUSSION

A. Equipment:

The equipment set up used for welding the samples is shown in Figure 1. The press is a converted Carver Laboratory Mounting Press. The pump gage indicates pounds per square inch of oil pressure and the force on the ram. As can be seen in Figure 1 the samples are held in alignment for welding by a special jig. This jig, Figure 2, uses a transite socket to insulate the sample from the main components of the jig. This insulation prevents the jig from becoming a heat sink, consequently it remained cool during the welding operation.

Heating of the samples during welding was accomplished by induction. The coil used, Figure 3, consisted of three turns of 1/8 inch O. D. copper tubing. The coil was produced by wrapping the tubing around a 0.700 inch diameter rod. This rod was also used to maintain the coil shape. Mica was used as an insulator between successive turns of the coil. The coil was powered by an electronic induction heater power source with an output of 1500 watts and an output frequency of 400 K. C., Figure 4.

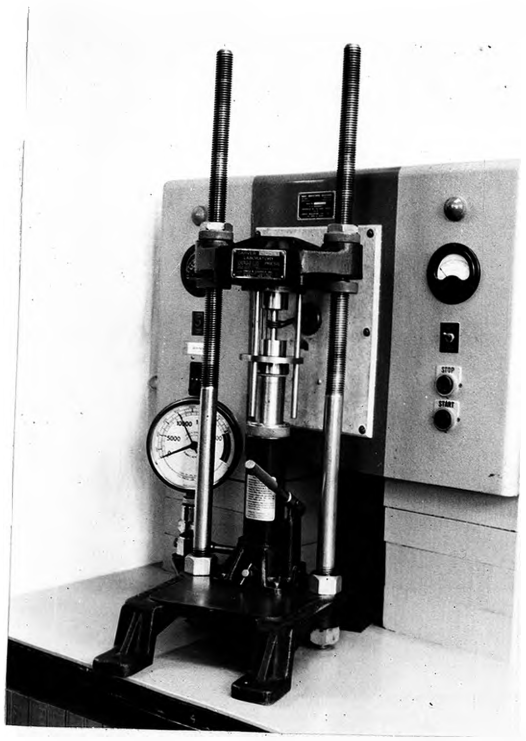

Figure 1. Equipment set up used for welding.

Figure 2. Sample holding jig.

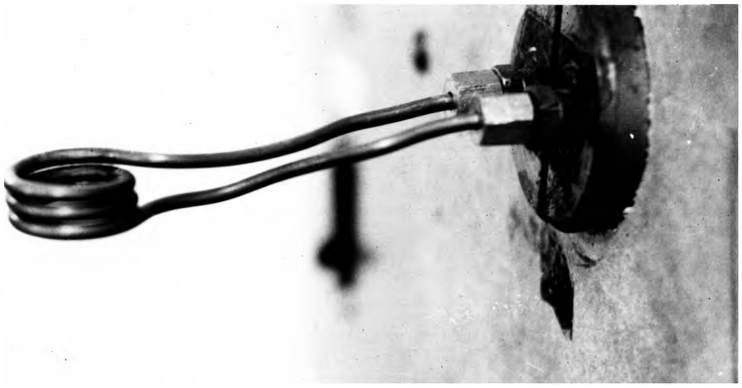

Figure 3. Induction coil.

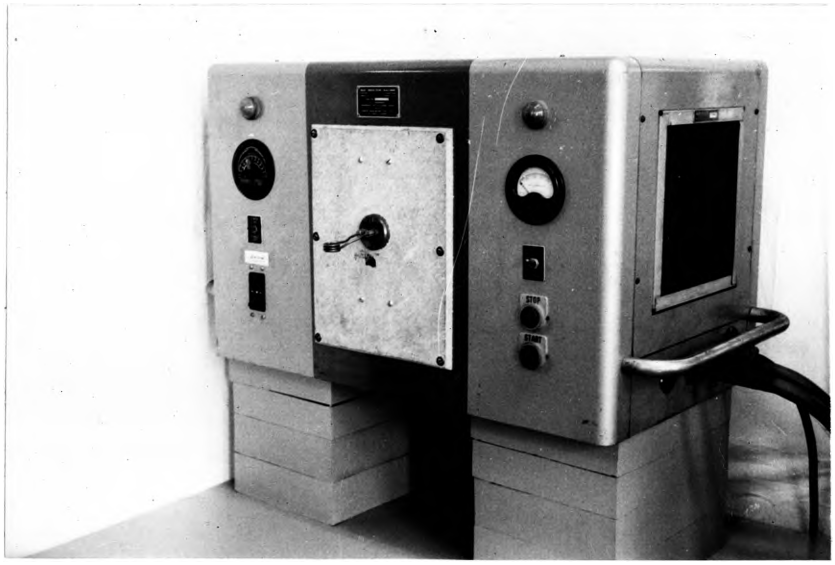

Figure 4. Electronic induction unit.

B. Welding Procedure:

The samples used in the welding operation were one half inch in diameter by two inches long. The nodular iron pieces were machined from continuous cast, one inch diameter, centerless ground, bar stock. The steel was S. A. E. 1018 cold rolled, one half inch diameter bar stock. Both the steel and the iron samples were cut to length and the ends faced on a lathe.

Prior to welding, the sample ends to be joined were mechanically cleaned using 180 grit emery paper. They were then immediately placed in the holding jig and centered in the coil. Care was taken to see that the interface was in the center of the coil. The required amount of end load was applied followed by the application of power to the coil which welded the samples. As the interface was heated the pressure first rose due to the expansion of the samples and then dropped as the heated zone deformed.

In order to avoid having a thermocouple inclusion at the interface of each test sample the time of heating at each end load was correlated with temperature, Figure 5. These curves were then used to determine the time required to obtain the welding temperature. The proper time was

FIGURE 5. TEMPERATURE VS. TIME CORRELATION

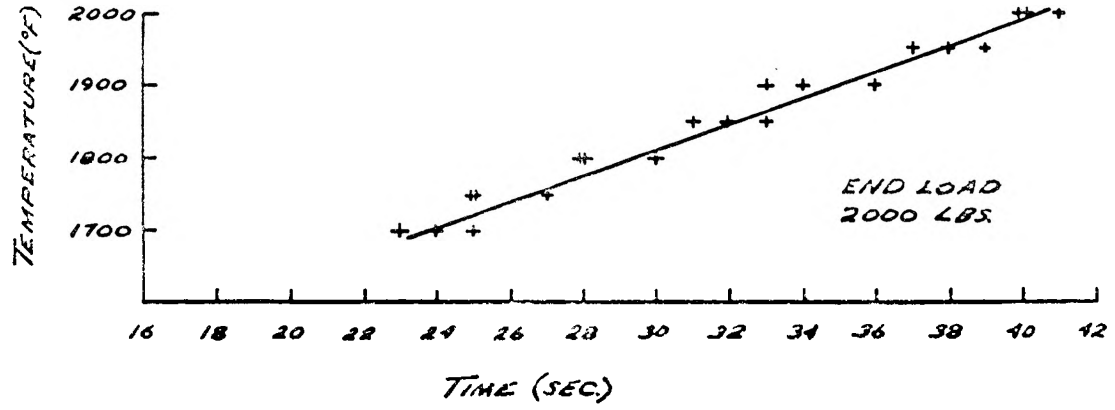

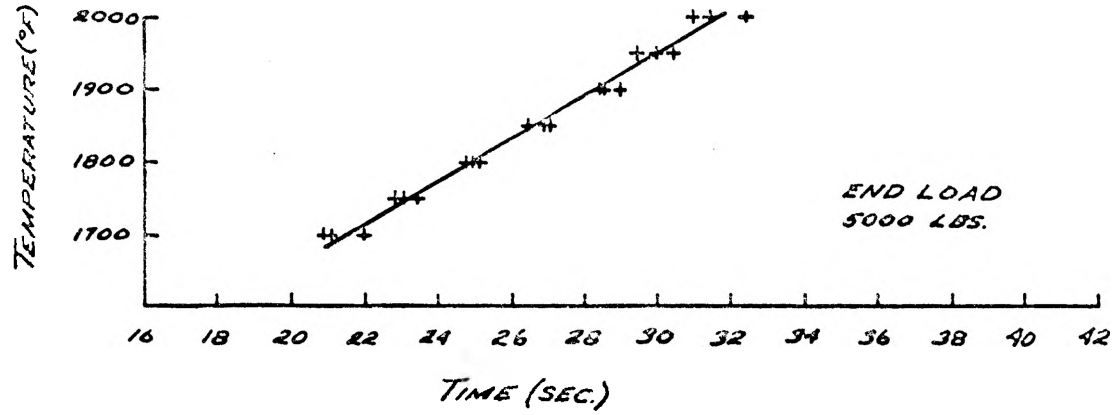

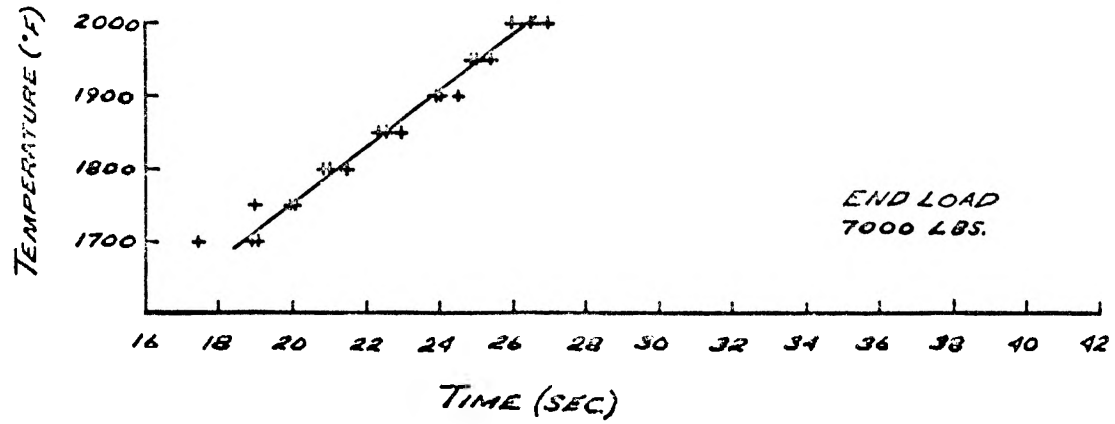

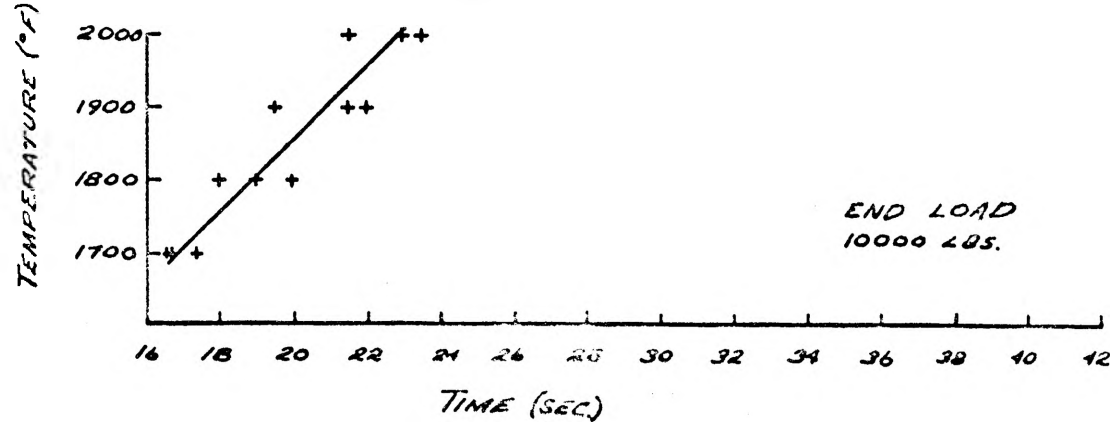

set on the automatic timer incorporated in the induction unit. This timer shut off the power to the coil after the set time elapsed. Test samples were produced at end loads of 2000 pounds (10,200 psi), 5000 pounds (25,500 psi), 7000 pounds (35,700 psi) and 10,000 pounds (51,000 psi) with temperature increasing in fifty degree increments from 1800°F to 2000°F. Four welds at each combination were produced. Examples of these welded samples can be seen in Figure 6: they represent each load, increasing to the right, welded at a temperature of 1850°F.

The diameter of the deformed section of each sample was measured and the percentage of area increase calculated, using the following equation:

$$\text{Deformation} = \text{Percent increase in area} = \frac{\text{Final Area - Initial Area}}{\text{Initial Area}} \times 100$$

These percentages are recorded in Tables I, II, III, IV, and V.

C. Testing:

Before the samples were tested in tension the deformed joint was machined to a diameter of one half inch, the same as the original stock. Three of the four samples at each temperature-pressure combination were tested to failure; this data is recorded in Tables I, II, III, IV,

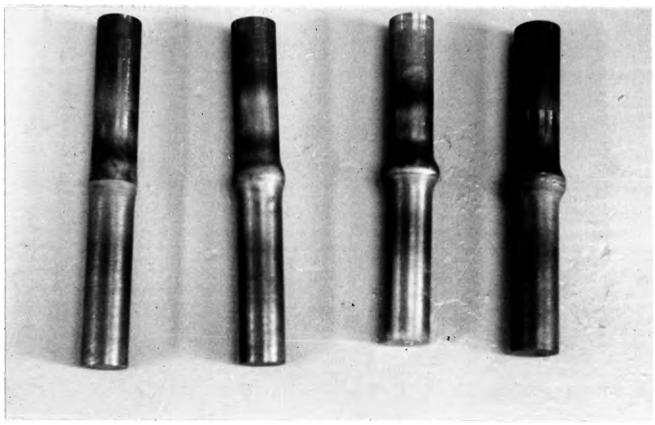

Figure 6. Examples of welded samples.

and V as the calculated ultimate tensile strength (pounds per square inch). The remaining sample in each group was sectioned, polished, etched and photomicrographs taken. The microstructures appear in Figures 10 thru 14. Microstructures of failures are shown in Figures 15 thru 18. These are representative of the types of failure which occurred.

D. Results:

The experimental results are tabulated in Tables I, II, III, IV and V and plotted in Figures 7, 8 and 9. From these it can be seen that as the end load increased at each temperature the strength increased to a maximum then decreased slightly. This can be explained in part by examination of the microstructures. The interface strength continues to increase with increasing pressure but there is also an increase in the deformation of the nodules in the iron. Examination of the photomicrographs taken of the failures, Figures 16, 17, 18, shows the lines of failure follow from one deformed graphite nodule to the next. In Figure 18 where the nodules are deformed nearly flat the line of failure is almost parallel to the interface. This is as one would expect since the severely flattened nodules create a very definite plane of possible failure. Because

the samples failed in the base material and not along the interface as did the 2000 pound end load example, Figure 15, it would be safe to assume that the interface bond has reached a strength that exceeds the strength of the heat and pressure affected iron.

Upon inspection of the heat affected zone of a typical weld the first observed structure change is the recrystallization of the distorted cold rolled ferrite grains in the steel. Progressing toward the interface the pearlite becomes more predominant until at the interface there is a layer containing only pearlite. This pearlite would indicate that there has been diffusion of carbon across the interface from the higher carbon concentration of the cast iron into the lower carbon concentration of the steel. The interface is plainly visible due to the distinct difference in the structure of the materials. Once across the interface into the iron, the ferrite and pearlite structure is mottled and the various loads deform it to different degrees. Progressing away from the interface it is noticeable that the amount of pearlite in the microstructure tends to decrease until once out of the heat affected zone the iron has its as-cast structure, Figure 19.

FIGURE 7. TENSILE STRENGTH VS. END LOAD

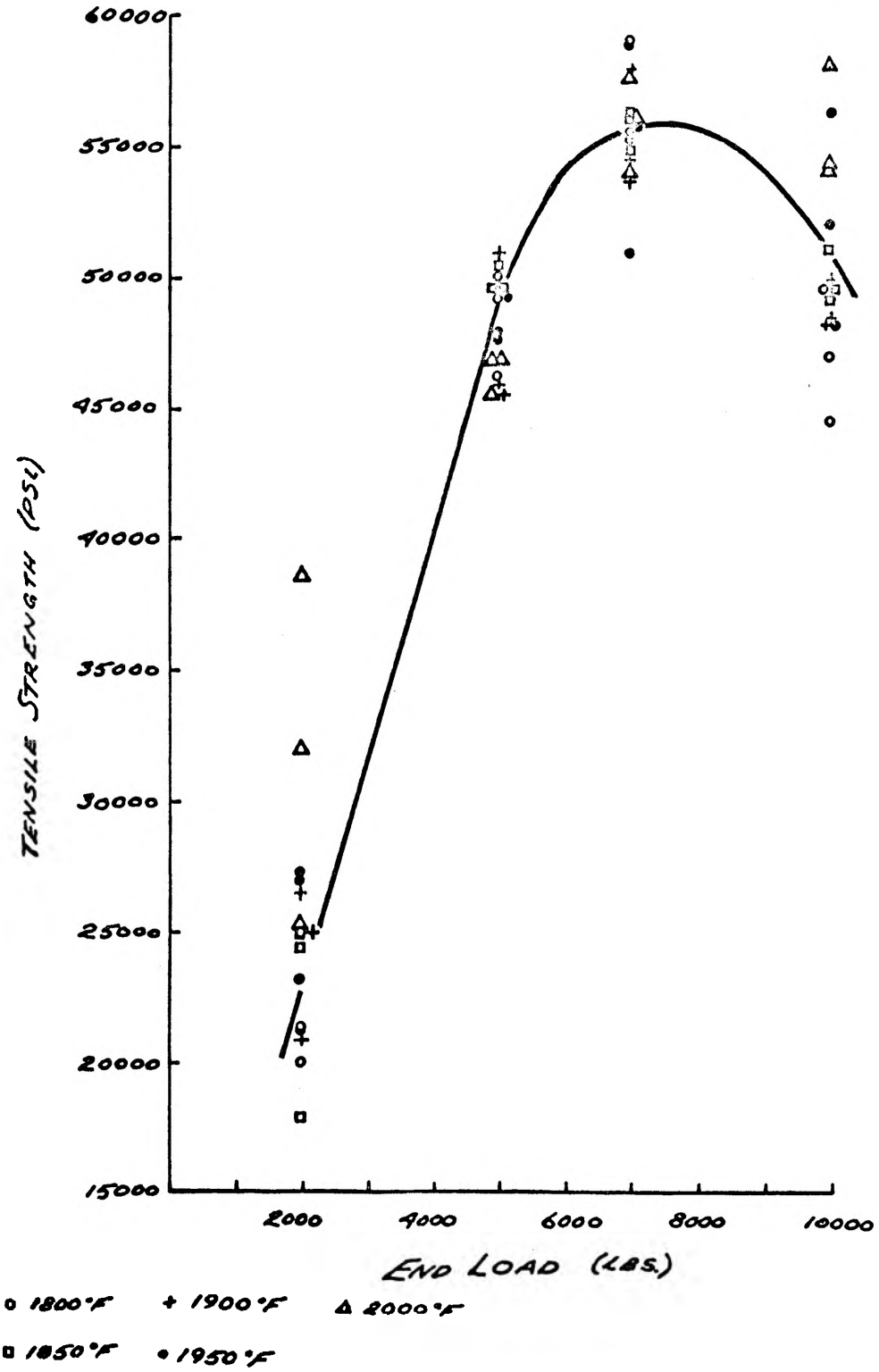

FIGURE 8. TENSILE STRENGTH VS. DEFORMATION

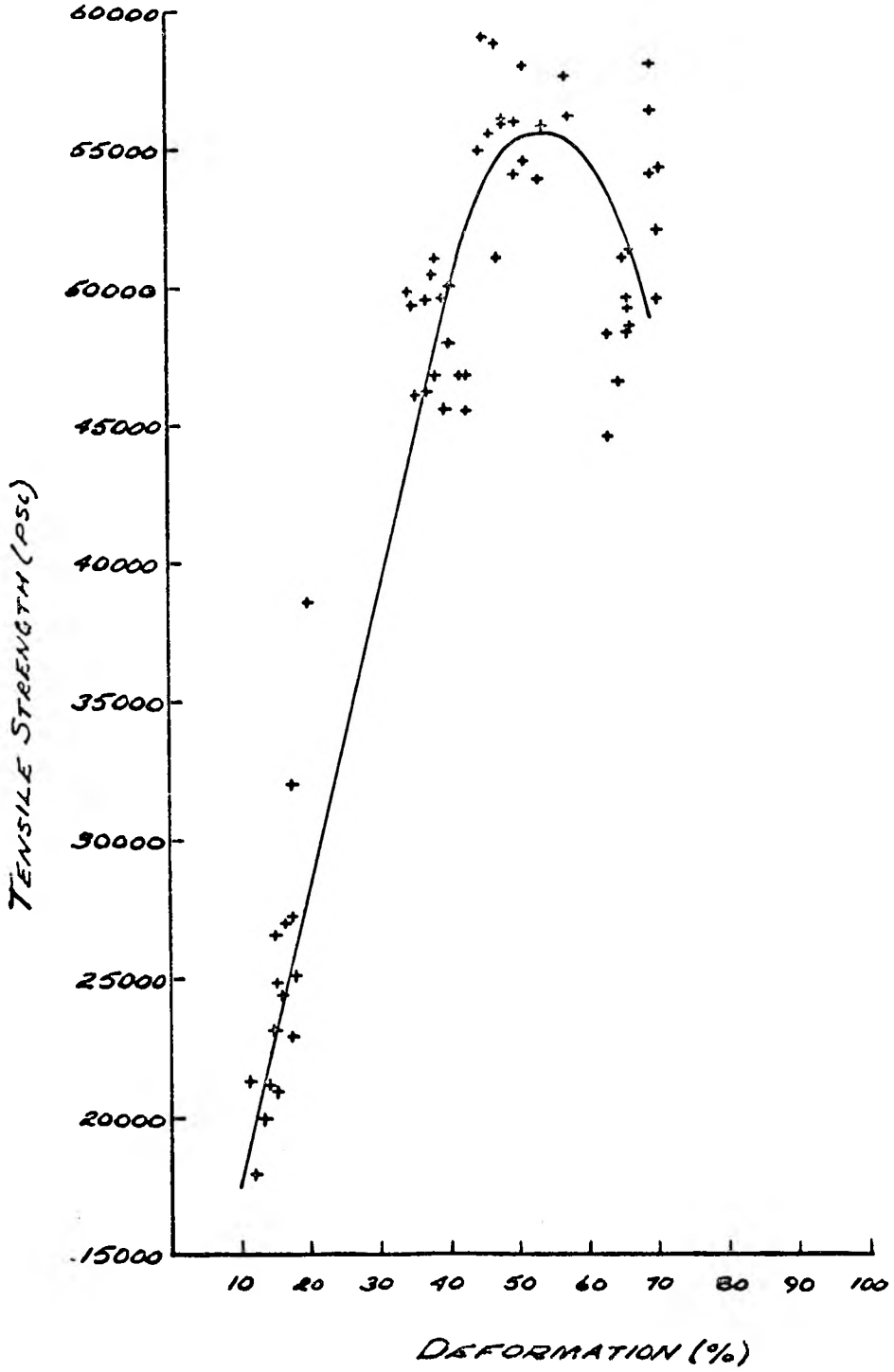

FIGURE 9. TENSILE STRENGTH VS. TEMPERATURE

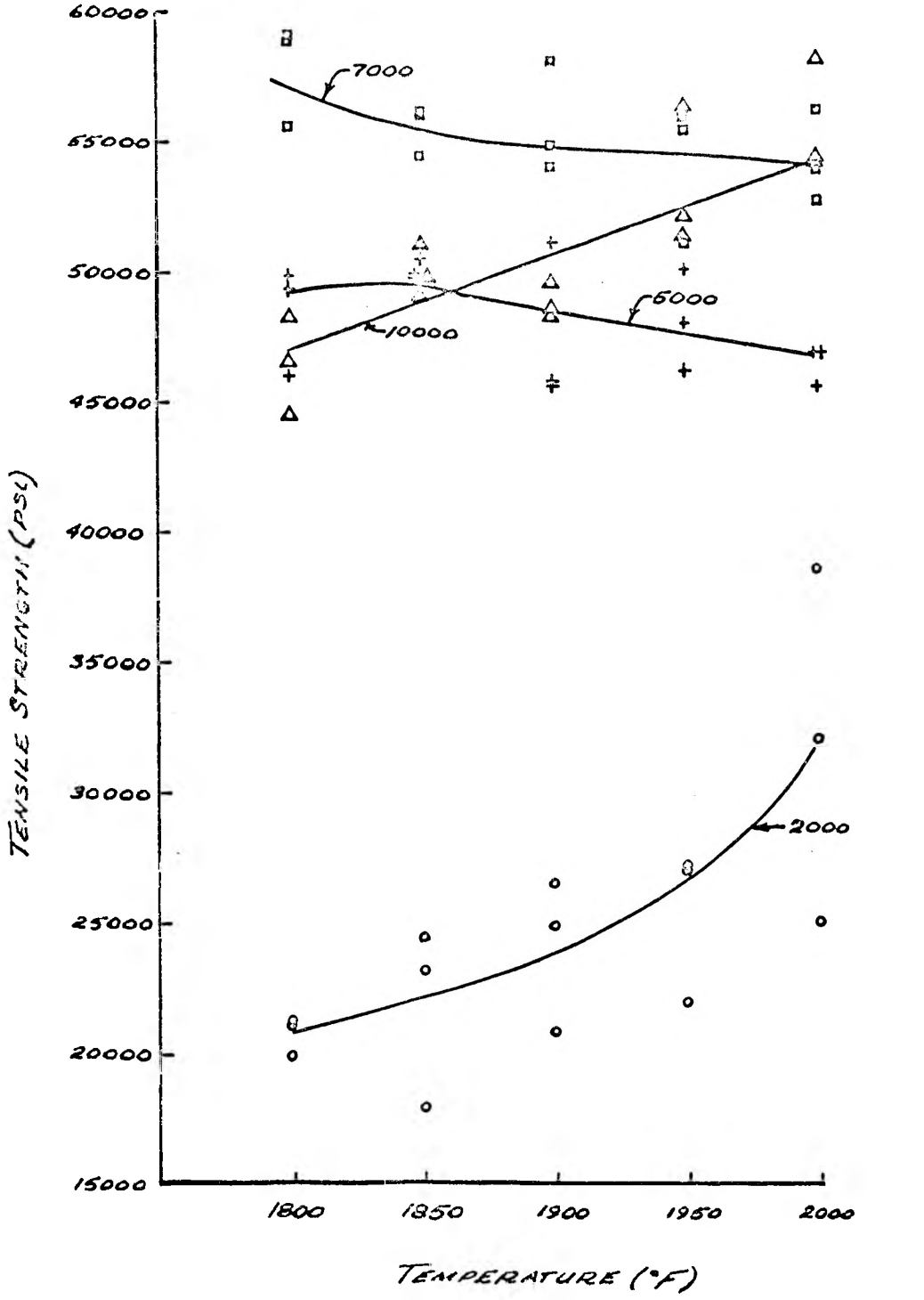

Table I. Experimental Data, Welding Temperature 1800°F.

Sample No.	Initial Load (lbs.)	(psi)	Deformation (%)	Tensile Strength (psi)	Failure Location
7	2,000	10,200	11.2	21,300	Interface
8	2,000	10,200	13.6	20,050	Interface
9	2,000	10,200	15.1		
10	2,000	10,200	14.0	21,200	Interface
27	5,000	25,500	34.8	49,800	Iron
28	5,000	25,500	36.0	46,000	Iron
29	5,000	25,500	35.2	49,300	Iron
30	5,000	25,500	36.8		
47	7,000	35,700	46.0	55,500	Iron
48	7,000	35,700	45.6	59,000	Iron
49	7,000	35,700	47.2	58,800	Iron
50	7,000	35,700	47.6		
67	10,000	51,000	64.8	46,500	Iron
68	10,000	51,000	63.2	48,300	Iron
69	10,000	51,000	62.0		
70	10,000	51,000	63.2	44,600	Iron

Figure 10. Microstructure Of Samples Welded At 1800°F. 200 X.

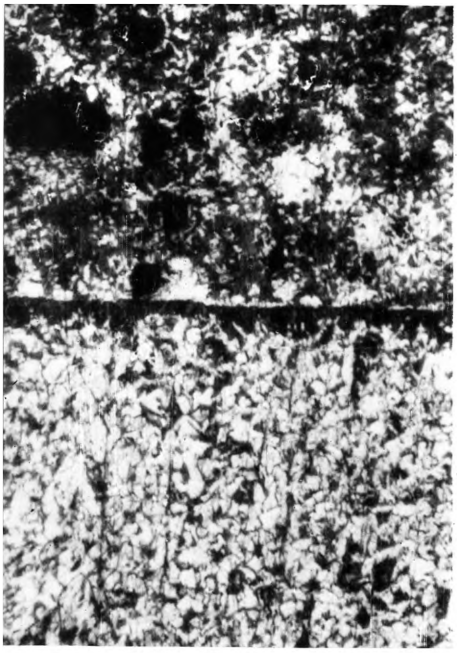

End load 2,000 pounds.

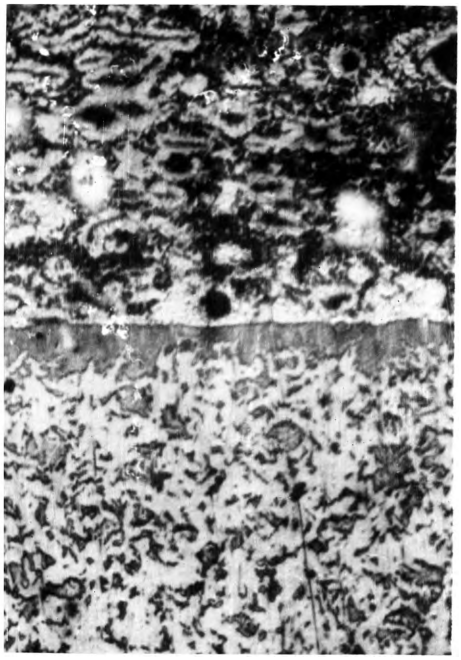

End load 5,000 pounds.

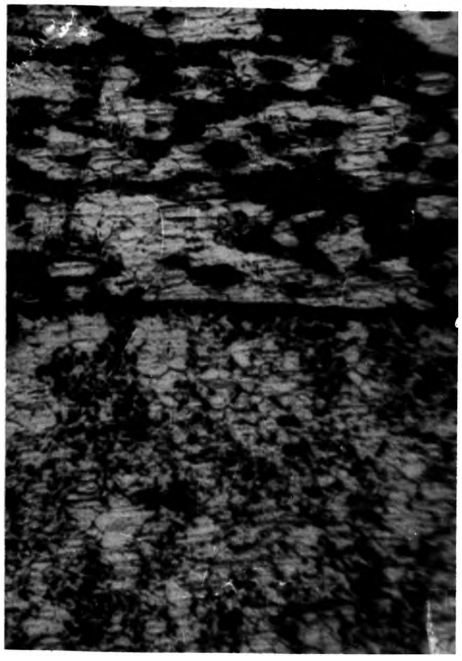

End load 7,000 pounds.

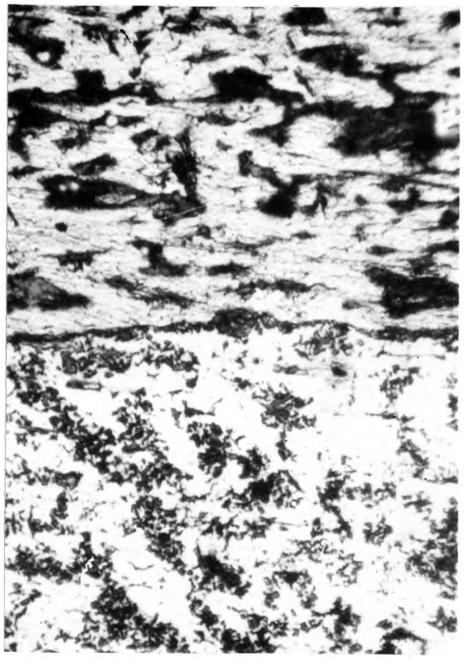

End load 10,000 pounds.

Table II. Experimental Data, Welding Temperature 1850°F.

Sample No.	Initial Load (lbs.)	(psi)	Deformation (%)	Tensile Strength (psi)	Failure Location
11	2,000	10,200	16.0	24,400	Interface
12	2,000	10,200	14.8	23,200	Interface
13	2,000	10,200	14.8		
14	2,000	10,200	12.0	17,900	Interface
31	5,000	25,500	38.8	50,400	Iron
32	5,000	25,500	37.6		
33	5,000	25,500	39.6	49,600	Iron
34	5,000	25,500	37.2	49,500	Iron
51	7,000	35,700	46.8		
52	7,000	35,700	51.2	54,400	Iron
53	7,000	35,700	48.8	56,000	Iron
54	7,000	35,700	50.0	55,900	Iron
71	10,000	51,000	66.0	49,200	Iron
72	10,000	51,000	65.6		
73	10,000	51,000	65.6	51,000	Iron
74	10,000	51,000	66.0	49,500	Iron

Figure 11. Microstructure Of Samples Welded At 1850°F. 200 X.

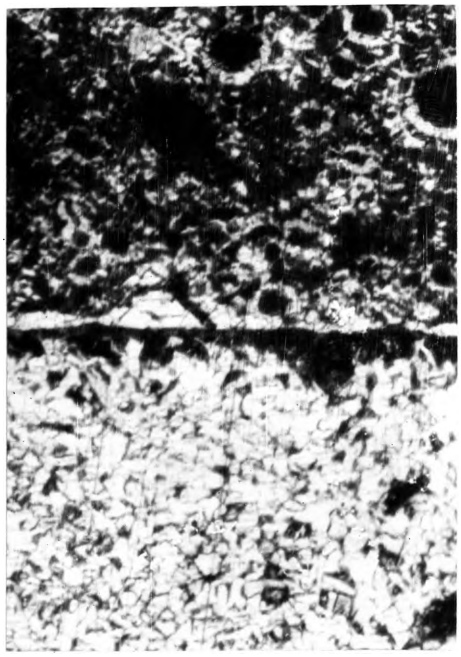

End load 2,000 pounds.

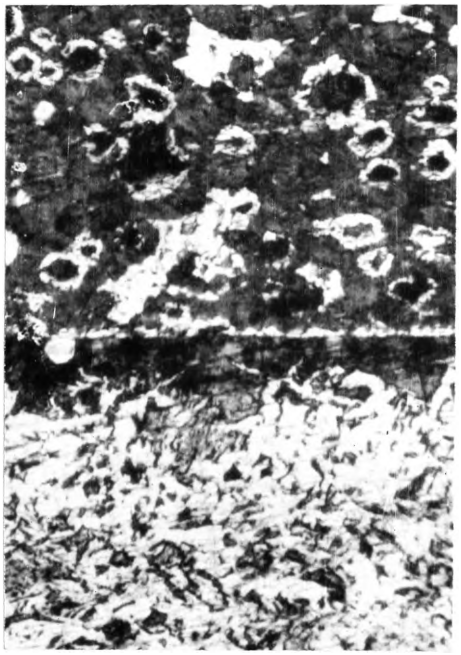

End load 5,000 pounds.

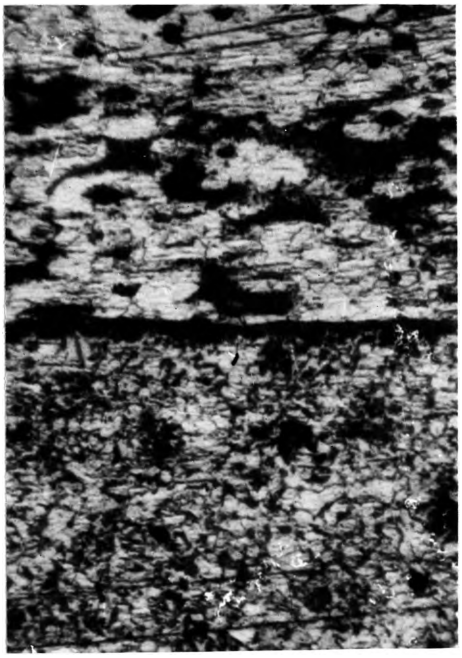

End load 7,000 pounds.

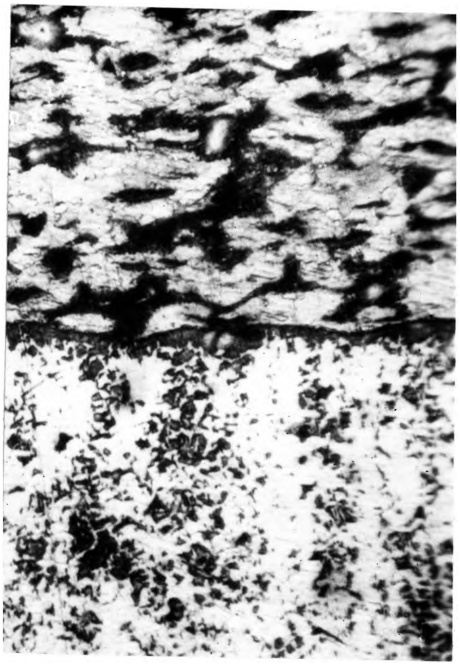

End load 10,000 pounds.

Table III. Experimental Data, Welding Temperature 1900°F.

Sample No.	Initial Load (lbs.)	(psi)	Deformation (%)	Tensile Strength (psi)	Failure Location
15	2,000	10,200	15.1	20,900	Interface
16	2,000	10,200	16.0		
17	2,000	10,200	15.1	26,600	Interface
18	2,000	10,200	15.1	24,900	Interface
35	5,000	25,500	40.0		
36	5,000	25,500	38.8	51,000	Iron
37	5,000	25,500	40.0	45,600	Iron
38	5,000	25,500	38.4	46,750	Iron
55	7,000	35,700	51.6	58,000	Iron
56	7,000	35,700	51.6		
57	7,000	35,700	50.0	53,900	Iron
58	7,000	35,700	44.8	54,800	Iron
75	10,000	51,000	66.0	48,300	Iron
76	10,000	51,000	66.4		
77	10,000	51,000	70.4	49,500	Iron
78	10,000	51,000	66.4	48,500	Iron

Figure 12. Microstructure Of Samples Welded At 1900°F. 200 X.

End load 2,000 pounds.

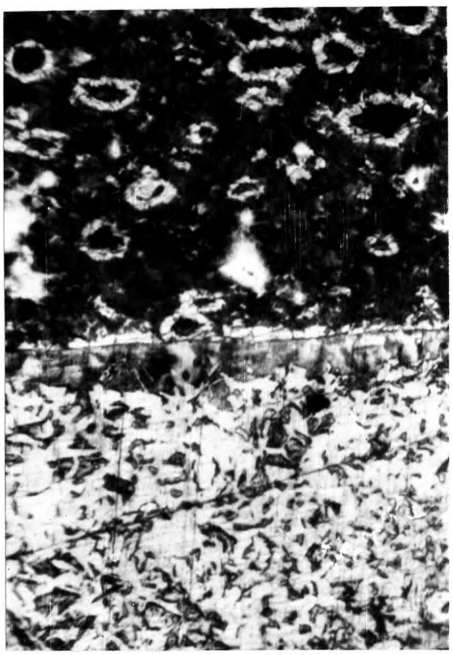

End load 5,000 pounds.

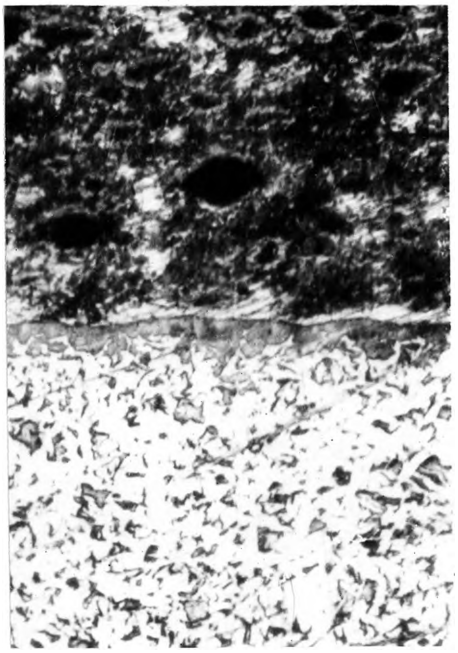

End load 7,000 pounds.

End load 10,000 pounds.

Table IV. Experimental Data, Welding Temperature 1950°F.

Sample No.	Initial Load (lbs.)	(psi)	Deformation (%)	Tensile Strength (psi)	Failure Location
19	2,000	10,200	17.6	27,200	Interface
20	2,000	10,200	16.8	27,000	Interface
21	2,000	10,200	17.6	22,900	Interface
22	2,000	10,200	15.1		
39	5,000	25,500	40.5	50,000	Iron
40	5,000	25,500	40.5	47,900	Iron
41	5,000	25,500	37.2	46,200	Iron
42	5,000	25,500	38.8		
59	7,000	35,700	47.6	51,000	Iron
60	7,000	35,700	54.0	55,300	Iron
61	7,000	35,700	48.4	55,800	Iron
62	7,000	35,700	46.8		
79	10,000	51,000	70.4		
80	10,000	51,000	69.6	56,300	Iron
81	10,000	51,000	66.4	51,300	Iron
82	10,000	51,000	70.4	52,000	Iron

Figure 13. Microstructure Of Samples Welded At 1950°F. 200 X.

End load 2,000 pounds.

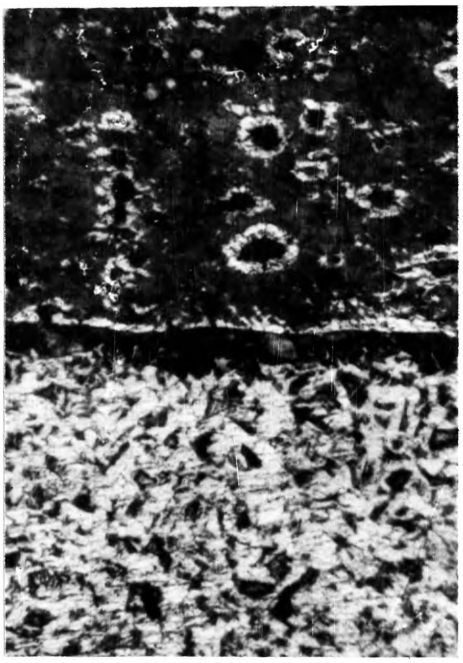

End load 5,000 pounds.

End load 7,000 pounds.

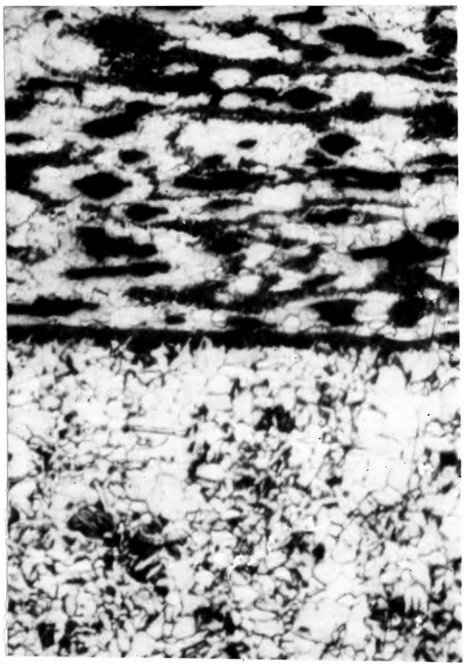

End load 10,000 pounds.

Table V. Experimental Data, Welding Temperature 2000°F.

Sample No.	Initial Load (lbs.)	(psi)	Deformation (%)	Tensile Strength (psi)	Failure Location
23	2,000	10,200	17.6	32,000	Interface
24	2,000	10,200	20.0	38,600	Interface
25	2,000	10,200	18.0	25,100	Interface
26	2,000	10,200	18.4		
43	5,000	25,500	42.0	46,800	Iron
44	5,000	25,500	42.8	45,600	Iron
45	5,000	25,500	42.0		
46	5,000	25,500	42.0	46,800	Iron
63	7,000	35,700	54.0		
64	7,000	35,700	58.0	56,100	Iron
65	7,000	35,700	53.2	53,800	Iron
66	7,000	35,700	57.6	57,600	Iron
83	10,000	51,000	69.6	58,000	Iron
84	10,000	51,000	69.3	54,000	Iron
85	10,000	51,000	70.8	54,200	Iron
86	10,000	51,000	70.8		

Figure 14. Microstructure Of Samples Welded At 2000°F. 200 X.

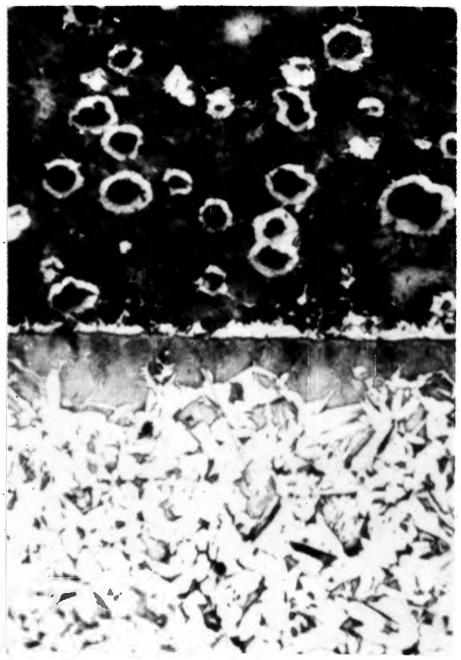

End load 2,000 pounds.

End load 5,000 pounds.

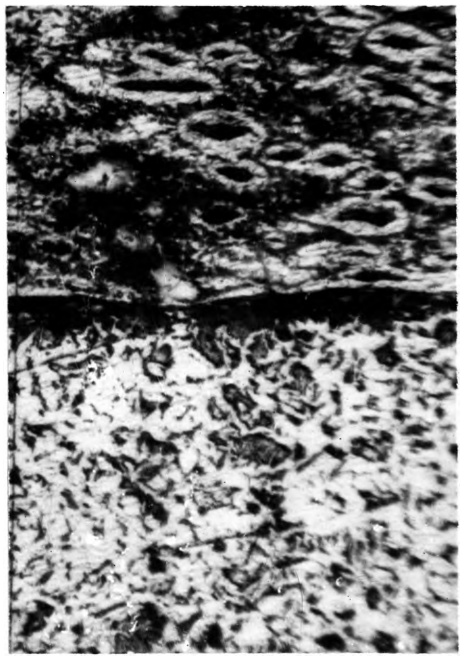

End load 7,000 pounds.

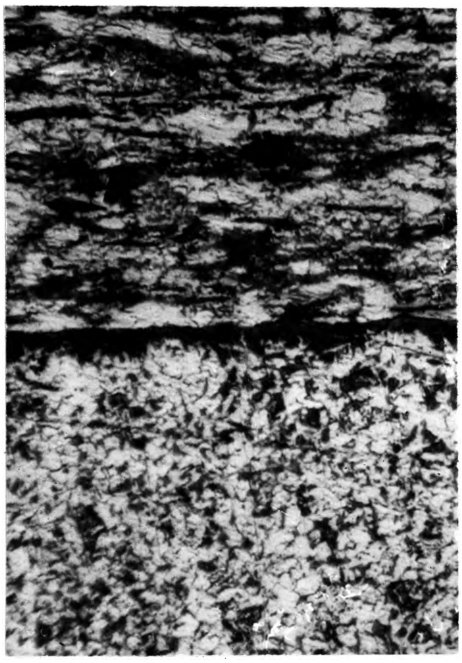

End load 10,000 pounds.

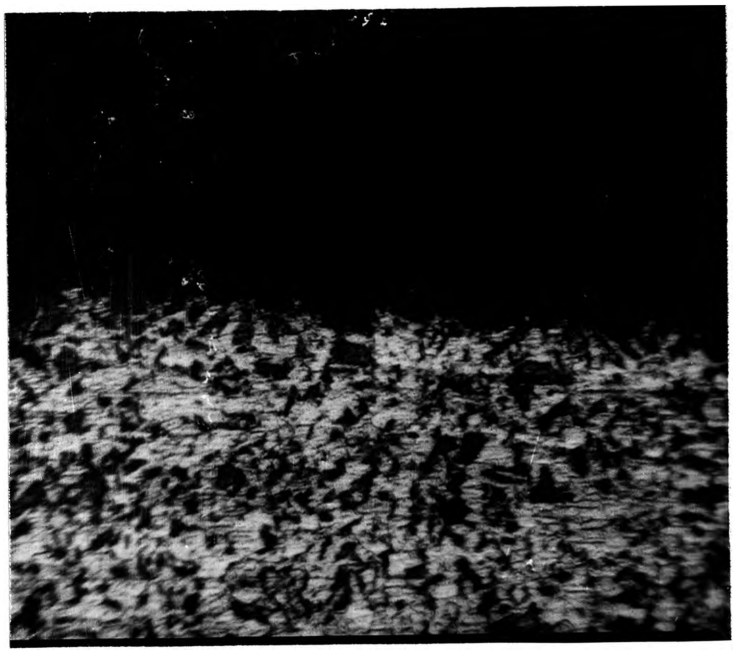

Figure 15. Photomicrograph of failure line, Sample No. 19. 200 X.

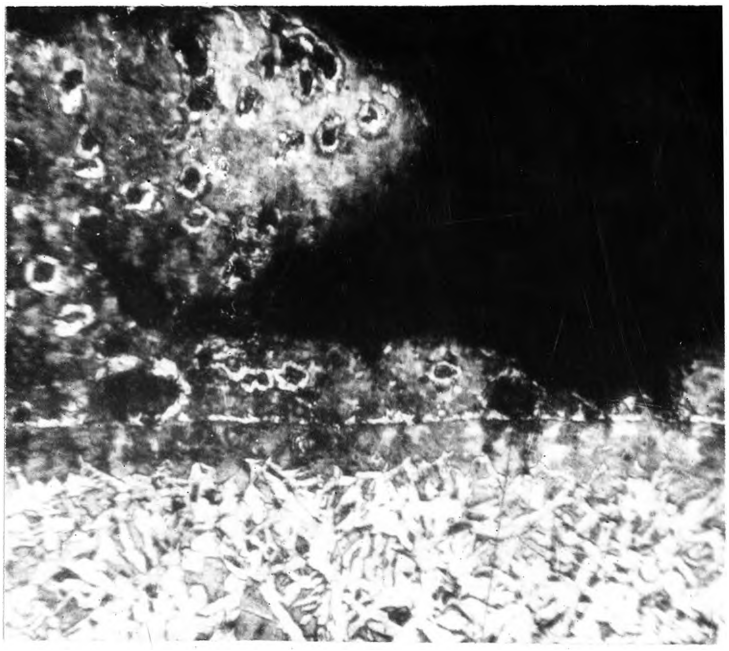

Figure 16. Photomicrograph of failure line, Sample No. 39. 200 X.

Figure 17. Photomicrograph of failure line, Sample No. 65. 200 X.

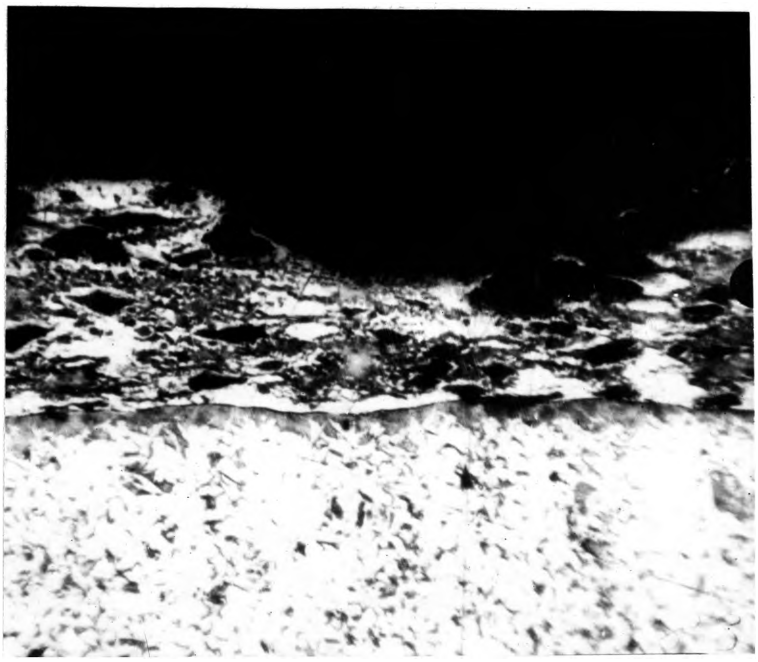

Figure 18. Photomicrograph of failure line, Sample No. 83. 200 X.

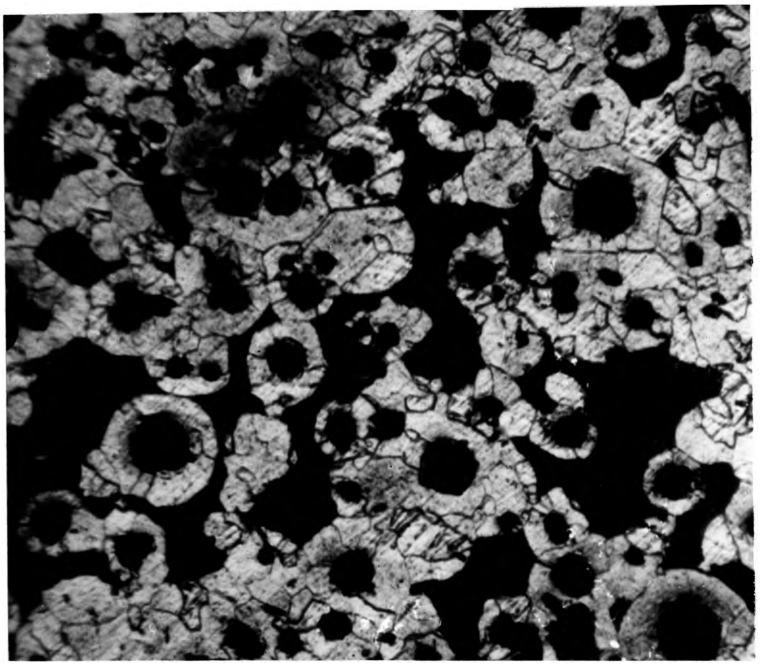

Figure 19. Microstructure of nodular iron, as received. 200 X.

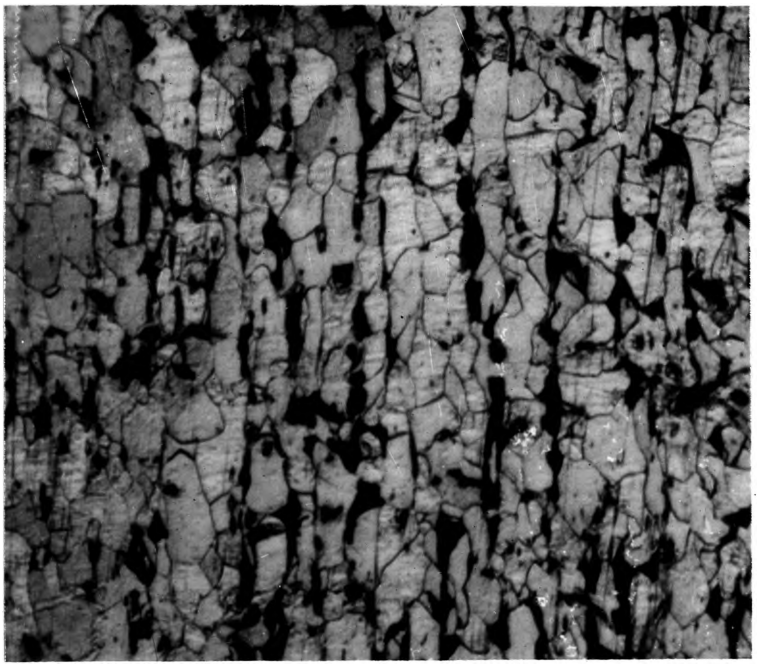

Figure 20. Microstructure of cold rolled S. A. E. 1018 steel bar, as received. 200 X.

IV. CONCLUSIONS

The experimental data shows that nodular iron can be welded to low carbon steel with reasonable strengths. The nodular iron used has an advertised strength of from 60,000 psi to 80,000 psi ultimate tensile strength. A sample of the stock used in the experiments exhibited a tensile strength of 69,800 psi. Using 60,000 psi as a minimum dependable strength, the strongest weld had a strength of 98.4 % of this value. The majority of the strongest welds are from 90 % to 95 % of this value. These welds of greatest strength are primarily in the group which were welded with 7000 pounds end load (35,700 psi), as can be seen in Figures 7 and 9. Figure 7 also shows clearly the decrease in weld strength due to the deformed graphite nodules in the iron. With these results it is apparent that the welds made at 7000 pounds end load (35,700 psi) have the greatest engineering value.

Pressure would seem to be the primary variable which effects the joint strength. Figures 7 and 9 show this clearly. They indicate that the increase in welding pressure is of greater importance than the increase in welding temperature. In Figure 9 this is apparent because

the individual curves at each pressure remain almost horizontal, although the 2000 pound and 10,000 pounds end load curves do rise slightly. This might be explained in that the higher temperature allowed for greater recrystallization and diffusion to occur thereby strengthening the joint and partially relieving the effects of the deformation. The photomicrographs show no indication of this effect.

Figure 8 shows a rise in ultimate tensile strength as the deformation is increased to the point where it is detrimental because of the deformation of the graphite nodules. Deformation, though, is a product primarily of pressure. An examination of the data will show the deformation to be about the same for all samples in each end load group. This is a result of the load being allowed to be reduced to zero during welding because of plastic deformation. As the sample was heated it deformed until the pressure was relieved and then the deformation remained about the same as the temperature increased. Therefore, using this method of welding, pressure and deformation will increase together, with deformation as a dependent variable.

The study of welding nodular iron to steel is at this point not complete. There are many mechanical properties of the welds yet unknown; fatigue strength, yield strength,

elongation, bend and impact strengths, should all be investigated. There is also the mechanism of diffusion of the oxide from the interface and the carbon across the interface. There is also the possibility of post-weld heat treatment, and the mechanical properties of the heat treated welds should be investigated.

BIBLIOGRAPHY

1. Kinzel, A. B. (1944) Adams Lecture--Solid-Phase Welding. Welding Journal, Vol. 28, p. 1124-1143.

2. Rollason, E. C. (1959) Pressure Welding of Metals. British Welding Journal, Vol. 6, p. 1-4.

3. General Electric Co. (1963) Diffusion Bonding Produces Invisible Joints. American Machinist Journal, Vol. 107, p. 163-164.

4. Fine, L., Maack, C. H. and Ozanick, A. R. (1946) Pressure Welding Part I. Metal Progress, Vol. 49, p. 350-365.

5. Holmes, E. (1959) Influence of Relative Interfacial Movement and Frictional Restraint In Cold Pressure Welding. British Welding Journal, Vol. 6, p. 29-37.

6. Nicholas, M. G. and Milner, D. R. (1961) Pressure Welding at Elevated Temperatures. British Welding Journal, Vol. 8, p. 375-383.

7. Vaidyanath, L. R. and Milner, D. R. (1960) Significance of Surface Preparation in Cold Pressure Welding. British welding Journal Vol. 7, p. 1-6.

8. Nicholas, M. G. and Milner, D. R. (1962) Roll Bonding of Aluminium. British Welding Journal, Vol. 9, p. 469-475.

9. Welding Handbook, 1960, Metals and Their Weldability. Fourth edition, Section Four, p. 69B.32.

10. McEwan, K. J. B. and Milner, D. R. (1962) Pressure Welding of Dissimilar Metals. British Welding Journal, Vol. 9, p. 406-420.

11. Tylecote, R. F. (1957) Pressure Welding in Practice. British Welding Journal, Vol. 4, p. 113-120.

12. Webb, W. (1962) 14-in. 138-K.V. Steel Pipe Production Line Butt Welding On Site. Electric World, Vol. 157, No. 26, p. 68-70.

13. Koppenhofer, R. L., Lewis, W. J., Faulkner, G. E., Rieppel, P. J., Cook, H. C. (1960) Induction-Pressure Welding of Girth Joints is Steel Pipe. Welding Journal, Vol. 49, p. 521-536.

14. Fine, L., Maack, C. H. and Ozanick, A. R. (1946) Pressure Welding Part II. Metal Progress Vol. 49, p. 521-536.

15. Lytle, A. R. (1944) Oxacetylene Pressure Welding. Welding Journal, Vol. 28, p. 1145-1151.

16. National Research Corporation (1963) Cold Welding: New Production Tool? Steel, Vol. 152, No. 24, p. 23.

17. Curtis, Frank W. (1944) High-Frequency Induction Heating. 1st. ed., McGraw Hill, New York. 235 p.

18. Davis, E. and Holmes, E. (1950) The Pressure-Welding Characteristics of Some Copper-Base Alloys. Journal of the Institute of Metals, Vol. 77, p. 185-206.

19. Guy, A. G. and Eiss, A. L. (1957) Diffusion Phenomeana In Pressure Welding. Welding Journal, Vol. 36, p. 473s-480s.

20. Donelan, J. A. (1959) Industrial Practice In Cold Pressure Welding. British Welding Journal, Vol. 6, p. 5-11.

21. Sliozberg, S. K. and Vniieso, S. K. (1961) Investigation of Metal Deformation in Pressure Butt Welding. Welding Production, No. 11, p. 3-10.

22. Plumtree, A. and Holmes, E. (1963) Fatigue Properties of Mild Steel Pressure Butt Welds. Journal of the Iron and Steel Institude, Vol. 201, p. 422-427.

VITA

The author was born on February 7, 1941 in St. Louis, Missouri. He received his primary and secondary education in St. Louis, Missouri. He received his college education from the University of Missouri School of Mines and Metallurgy at Rolla, Missouri and was graduated with a Bachelor of Science Degree in Mechanical Engineering in May, 1963.

He has been enrolled in the Graduate School of the University of Missouri School of Mines and Metallurgy since January, 1963, and has held a Graduate Assistantship in the Metallurgical Engineering Department from September, 1963 to June, 1964.